

# Design of low-loss and highly birefringent hollow-core photonic crystal fiber

**Roberts, Peter John; Williams, D.P.; Sabert, H.; Mangan, Brian Joseph; Bird, D.M.; Birks, T.A.; Knight, J.C.; Russell, P.St.J.**

*Published in:*
Optics Express

*Link to article, DOI:*
10.1364/OE.14.007329

*Publication date:*
2006

*Document Version*
Publisher's PDF, also known as Version of record

# Design of low-loss and highly birefringent hollow-core photonic crystal fiber

**P. J. Roberts[1,2], D. P. Williams[1], H. Sabert[1], B. J. Mangan[1,2], D. M. Bird[3], T. A. Birks[1,3], J. C. Knight[3] and P. St. J. Russell[4]**

[1] *BlazePhotonics Ltd, University of Bath Campus, Claverton Down, Bath BA2 7AY, United Kingdom*

[2] *Department of Communications, Optics and Materials, Danish Technical University, DK-2800 Kgs. Lyngby, Denmark*

[3] *Department of Physics, University of Bath, Claverton Down, Bath BA2 7AY, United Kingdom.*

[4] *Institute for Optics, Information and Photonics, University of Erlangen-Nuremberg, Guenther-Scharowsky-Str. 1 D-91058, Erlangen, Germany*

pjr@com.dtu.dk

**Abstract:** A practical hollow-core photonic crystal fiber design suitable for attaining low-loss propagation is analyzed. The geometry involves a number of localized elliptical features positioned on the glass ring that surrounds the air core and separates the core and cladding regions. The size of each feature is tuned so that the composite core-surround geometry is antiresonant within the cladding band gap, thus minimizing the guided mode field intensity both within the fiber material and at material / air interfaces. A birefringent design, which involves a 2-fold symmetric arrangement of the features on the core-surround ring, gives rise to wavelength ranges where the effective index difference between the polarization modes is larger than $10^{-4}$. At such high birefringence levels, one of the polarization modes retains favorable field exclusion characteristics, thus enabling low-loss propagation of this polarization channel.



**OCIS codes:** (060.2310) Fiber optics; (060.2400) Fiber properties; (060.2420) Fibers, polarization-maintaining

## References and links

1. T. A. Birks, P. J. Roberts, P. St. J. Russell, D. M. Atkin, and T. J. Shepherd, "Full 2D photonic band gaps in silica/air structures," Electron. Lett. **31**, 1941-1943 (1995).
2. R. F. Cregan, B. J. Mangan, J. C. Knight, T. A. Birks, P. St. J. Russell, P. J. Roberts, and D. C. Allan, "Single-mode photonic band gap guidance of light in air," Science **285**, 1537-1539 (1999).
3. D. G. Ouzounov, F. R. Ahmad, D. Muller, N. Venkataraman, M. T. Gallagher, M. G. Thomas, J. Silcox, K. W. Koch, and A. L. Gaeta, "Generation of megawatt optical solitons in hollow-core photonic band-gap fibers," Science **301**, 1702-1704 (2003).
4. J. Limpert, T. Schriedber, S. Nolte, H. Zellmer, and A. Tunnermann, "All fiber chirped-pulse amplification system based on compression in air-guiding photonic band gap fiber," Opt. Express **11**, 3332-3337 (2003).
5. C. J. S. de Matos, J. R. Taylor, T. P. Hansen, K. P. Hansen, and J. Broeng, "All-fiber chirped pulse amplification using highly dispersive air-core photonic band gap fiber," Opt. Express **11**, 2832-2837 (2003).
6. G. Humbert, J. C. Knight, G. Bouwmans, P. St. J. Russell, D. P. Williams, P. J. Roberts, and B.J. Mangan, "Hollow core photonic crystal fibers for beam delivery," Opt. Express **12**, 1477-1484 (2004).
7. F. Benabid, F. Couny, J. C. Knight, T. A. Birks, and P. St. J. Russell, "Compact, stable and efficient all-fibre gas cells using hollow-core photonic crystal fibres," Nature **434**, 488-491 (2005).
8. F. Benabid, P. Light, F. Couny, and P. St. J. Russell, "Electromagnetically-induced transparency grid in acetylene-filled hollow-core PCF," Opt. Express **13**, 5694-5703 (2005).
9. G. Bouwmans, F. Luan, J. C. Knight, P. St. J. Russell, L. Farr, B. J. Mangan, and H. Sabert, "Properties of a hollow-core photonic bandgap fiber at 850nm wavelength," Opt. Express **14**, 1613-1620 (2003).
10. X. Chen, M. J. Li, N. Venkataraman, M. Gallagher, W. Wood, A. Crowley, J. Carberry, L. Zenteno, and K. Koch, "Highly birefringent hollow-core photonic bandgap fiber," Opt. Express **12**, 3888-3893 (2004).
11. M. Wegmuller, M. Legré, N. Gisin, T. P. Hansen, C. Jakobsen, and J. Broeng, "Experimental investigation of the polarization properties of a hollow core photonic bandgap fiber for 1550 nm," Opt. Express **13**, 1457-1467 (2005).

#71838 - $15.00 USD Received 9 June 2006; revised 25 July 2006; accepted 26 July 2006

12. K. Saitoh and M. Koshiba, "Photonic bandgap fibers with high birefringence," IEEE Photon. Technol. Lett. **14**, 1291-1293 (2002).
13. F. Poletti, N. G. R. Broderick, D. J. Richardson, and T. M. Monro, "The effect of core asymmetries on the polarization properties of hollow core photonic bandgap fibers," Opt. Express **13**, 9115-9124 (2005).
14. J. A. West, C. M. Smith, N. F. Borrelli, D. C. Allan, and K. W. Koch, "Surface modes in air-core photonic band-gap fibers," Opt. Express **12**, 1485-1496 (2004).
15. P. J. Roberts, F. Couny, H. Sabert, B. J. Mangan, D. P. Williams, L. Farr, M. W. Mason, A. Tomlinson, T. A. Birks, J. C. Knight, and P. St. J. Russell, "Ultimate low loss of hollow-core photonic crystal fibers," Opt. Express **13**, 236-244 (2005).
16. P. J. Roberts, D. P. Williams, B. J. Mangan, H. Sabert, F. Couny, W. J. Wadsworth, T. A. Birks, J. C. Knight, and P. St. J. Russell, "Realizing low loss air core photonic crystal fibers by exploiting an antiresonant core surround," Opt. Express **13**, 8277-8285 (2005).
17. B. J. Mangan, L. Farr, A. Langford, P. J. Roberts, D. P. Williams, F. Couny, M. Lawman, M. Mason, S. Coupland, R. Flea, H. Sabert, T. A. Birks, J. C. Knight, and P. St. J. Russell, "Low loss (1.7 dB/km) hollow core photonic band gap fibre," Proc. Conf. Optical Fiber Commun., paper PDP24 (Los Angeles, 2004).
18. N. M. Litchinitser, A. K. Abeeluck, C. Headley, and B. J. Eggleton, "Antiresonant reflecting photonic crystal optical waveguides," Opt. Lett. **27**, 1592-1594 (2002).
19. N. M. Litchinitser, S. C. Dunn, B. Usner, B. J. Eggleton, T. P. White, R. C. McPhedran, and C. M. de Sterke, "Resonances in microstructured optical waveguides," Opt. Express **11**, 1243-1251 (2003).
20. P. Yeh, A. Yariv and E. Marom, "Theory of Bragg fiber," J. Opt. Soc. Am. **68**, 1196-1201 (1978).
21. T. P. White, B. T. Kuhlmey, R. C. McPhedran, D. Maystre, G. Renversez, C. M. de Sterke, and L. C. Botten, "Multipole method for microstructured optical fibers: 1. Formulation," J. Opt. Soc. Am. B **19**, 2322-2330 (2002).
22. P. J. Roberts and T. J. Shepherd, "The guidance properties of multi-core photonic crystal fibres," J. Optics A: Pure and applied **3**, S133-S140 (2001).
23. A. W. Snyder and J. D. Love, *Optical Waveguide Theory* (Chapman and Hall, London, 1983).
24. N. Guan, S. Habu, K. Takenaga, K. Himeno, and A. Wada, "Boundary element method for analysis of holey optical fibers," J. Lightwave Technol. **21**, 1787-1792 (2003).
25. C. M. Smith, N. Venkataraman, M. T. Gallagher, D. Müller, J. A. West, N. F. Borrelli, D. C. Allan, and K. W. Koch, "Low-loss hollow-core silica/air photonic bandgap fibre," Nature **424**, 657-659 (2003).
26. N. A. Mortensen and M. D. Nielsen, "Modeling of realistic cladding structures for air-core photonic band-gap fibers," Opt. Lett. **29**, 349-351 (2004).
27. S. G. Johnson and J. D. Joannopoulos, "Block-iterative frequency-domain methods for Maxwell's equations in a planewave basis," Opt. Express **8**, 173-190 (2001).

## 1. Introduction

Hollow core photonic crystal fibers (HC-PCFs), which guide light due to the presence of a photonic bandgap [1, 2], enable high-power light delivery in a single spatial mode. Since very low nonlinearity is ensured by most of the light being confined to the hollow core, the mode area can be relatively small, a typical size being around $40\lambda^2$ where $\lambda$ is the optical wavelength. This allows an extremely high power-density at the fiber output and also implies resilience to bend-induced mode coupling which would otherwise degrade the output beam profile, increase loss and potentially cause fiber damage due to an increased power overlap with the glass. As well as for high-power light delivery [3-6], HC-PCFs have been used in sensor and nonlinear-optics [7, 8] applications in which a gas is introduced into the core region. The fibers are naturally suited to these uses due to the long interaction lengths and small modal areas that are readily attainable, together with a large overlap between the gas and the guided mode.

In many applications a polarization-maintaining HC-PCF is either preferred or required. The presence of uncontrolled birefringence or polarization mode dispersion (PMD) can severely limit the pulse compression attainable in a communication or other pulse-delivery system, and will also severely degrade the performance in interferometric applications. The measured birefringence of fabricated HC-PCF has been found to be large, to vary rapidly with wavelength, and to be accompanied with a high degree of polarization dependent loss (PDL) [9-11]. Polarization dependent behavior is manifest even if the fiber is not intentionally birefringent due to the inevitable geometric distortions which arise when HC-PCFs are drawn [9, 11]. Numerical investigations have confirmed the birefringence properties are very sensitive to the fiber geometry [12], and particularly to any deformations in the glass ring

#71838 - $15.00 USD Received 9 June 2006; revised 25 July 2006; accepted 26 July 2006

which surrounds the hollow core [13]. High birefringence and PDL is associated with a polarization-splitting in the wavelengths at which anti-crossing events occur between a core guided mode and modes associated with the core-surround ring [13,14]. The polarized core mode which is close to anti-crossing with a core-surround mode possessing compatible symmetry suffers a significant effective index change and more of its field overlaps with the glass. An associated increase in the field overlap with the glass / air interfaces causes an increase in the loss suffered by this polarization mode.

Given the generic high birefringence of HC-PCF caused even by small symmetry-breaking geometrical perturbations, there is clearly the need to develop low-loss intentionally birefringent fibers which show a high degree of polarization maintenance. Low-loss guidance can be facilitated by the incorporation of antiresonant features within the core-surround. A non-birefringent antiresonant core-surround design, which is just a glass ring of appropriately chosen thickness, has been shown to substantially decrease the field intensity at the glass / air interfaces and therefore the loss [15, 16]. A fabricated fiber which incorporates a core-surround which is a close approximation to this geometry has shown losses as low as 1.2dB/km [15, 17]. In section 2 of the current paper, an alternative core-surround geometry is considered which incorporates a number of elliptical features on a thin core-surround ring. The elliptical form was chosen since it is approximates a shape which is compatible with the surface tension forces which act during the fiber draw if an appropriate fiber perform is used. The considered geometry is thus of a practical form for fabrication using a standard fiber drawing procedure. The size of the localized features is tuned so that the composite core-surround geometry is antiresonant within the cladding band-gap at the air light-line. This form of core-surround mimics an arrangement of Anti-Resonant Reflective Optical Waveguides (ARROW) which enclose a central core [18, 19], although the influence of the connecting ring of glass needs to be taken into account. Arrangements of the elliptical features which break 3-fold rotational symmetry introduce birefringence. One such arrangement is analyzed in section 3 and is found to possess wavelength ranges over which a high degree of birefringence is maintained, with one polarization channel predicted to guide with low-loss and the other with higher loss. Section 4 summarizes the results and draws some conclusions.

## 2. Antiresonant core-surround geometry for low-loss

A glass ring of constant thickness, tuned to antiresonance, is not the optimum geometry for achieving confinement. Before considering a practical geometry suitable for the core-surround incorporated within a HC-PCF, it is instructive to compare the ring geometry with a number of dielectric cylinders which enclose a central air core. In the latter case, the cylinders can be tuned to antiresonance to form an ARROW geometry [18, 19]. Two core sizes will be considered in the comparison, one being similar to the core size of a HC-PCF in which 7 unit cells are omitted in forming the core, and the other similar to a 19-cell core size.

Figure 1 schematically shows the considered geometries. The performance of a silica ring of thickness $t$ and radius $R$ will be compared to arrangements of cylinders evenly distributed around a circle of radius $R$. Collections of both 6 and 12 cylinders will be analysed as these arrangements are commensurate with the 6-fold symmetry of the archetypal HC-PCF. The ring thickness $t$ and the cylinder diameter $d$ can be tuned to antiresonance at a common wavelength $\lambda$. For definiteness $\lambda$=1.55μm will be chosen to set the scale.

#71838 - $15.00 USD Received 9 June 2006; revised 25 July 2006; accepted 26 July 2006

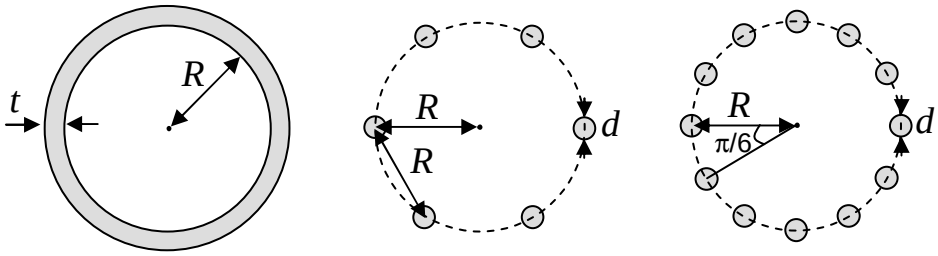


Fig. 1. Schematic representation of the considered geometries.

The chosen simplified geometries have the merit of being quick and easy to model, and serve to motivate the more detailed modeling work presented later. The ring geometry is analyzed using a transfer matrix approach [20] and the cylinder system using a multipole method [21, 22].

Figure 2 compares the confinement loss of the $HE_{11}$-like leaky modes of the geometries, at the core radii $R$=6μm and $R$=10μm appropriate to a 7-cell core and a 19-cell core, respectively. The confining ability of the cylinder ARROW geometries is superior to that of the continuous ring at each core size. At the smaller core size, 6 cylinders outperform 12 cylinders, but the situation is reversed at the larger core size. This can be interpreted as a minimum separation between the cylinders being required to prevent the light from resolving the gaps. The light will resolve a gap larger than about λ'/2, where λ' is the in-plane wavelength in air given by $\lambda' = \lambda / \left(1 - n^2\right)^{1/2}$ with $n$ the mode effective index. The peaks occurring beyond $d$=1.2μm for the cylinder-based geometries and at 0.74μm together with 1.48μm for the ring geometries correspond to resonances of these structures.

#71838 - $15.00 USD Received 9 June 2006; revised 25 July 2006; accepted 26 July 2006

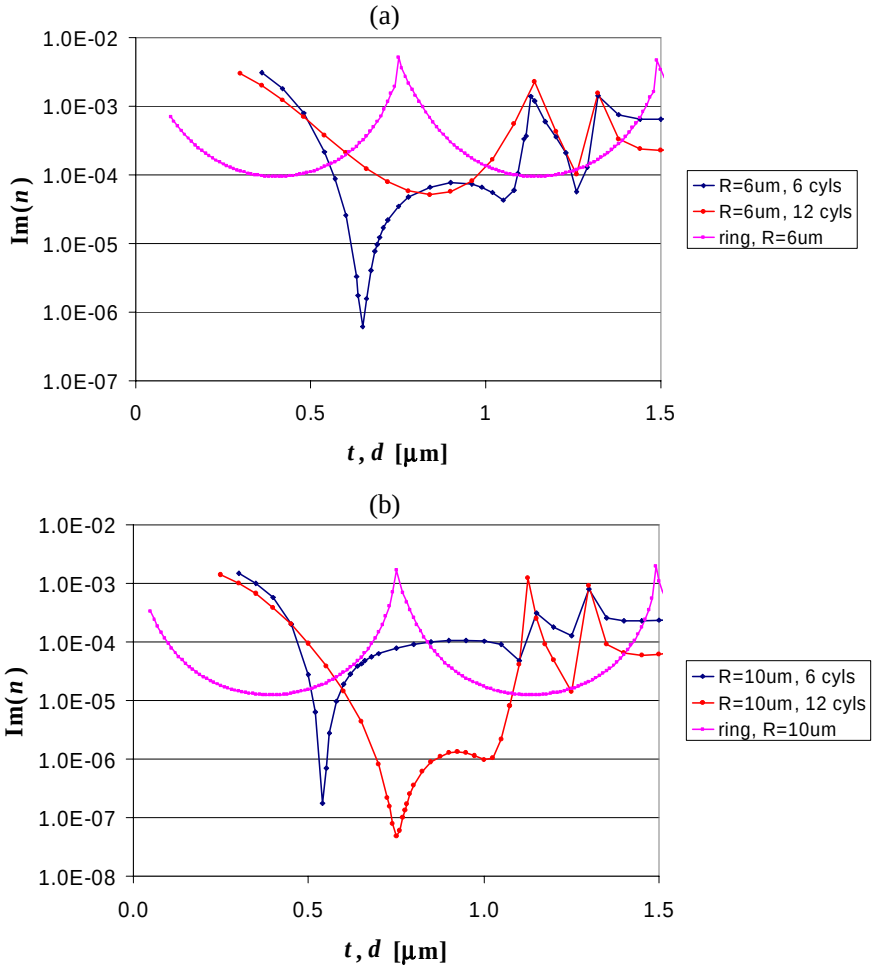


Fig. 2. The light confining ability of the simplified core-surround geometries.

A comparison of the normalized field intensity existing at the glass / air interfaces can be based on the quantity [15]

$$F = \left(\frac{\varepsilon_0}{\mu_0}\right)^{1/2} \frac{\oint_{\text{interfaces}} ds\,|\mathbf{E}|^2}{\left|\int_{A_c} dS\,(\mathbf{E}\wedge\mathbf{H})\cdot\hat{\mathbf{z}}\right|} \tag{1}$$

where, following [23], the area integration in the normalizing denominator term needs to be deformed into the complex plane due to the leaky nature of the modes. Figure 3 shows F for the geometries at the two core sizes. The minimum value of F obtained for the cylinder ARROW and the antiresonant ring geometries are remarkably similar at a common core size.

#71838 - $15.00 USD Received 9 June 2006; revised 25 July 2006; accepted 26 July 2006

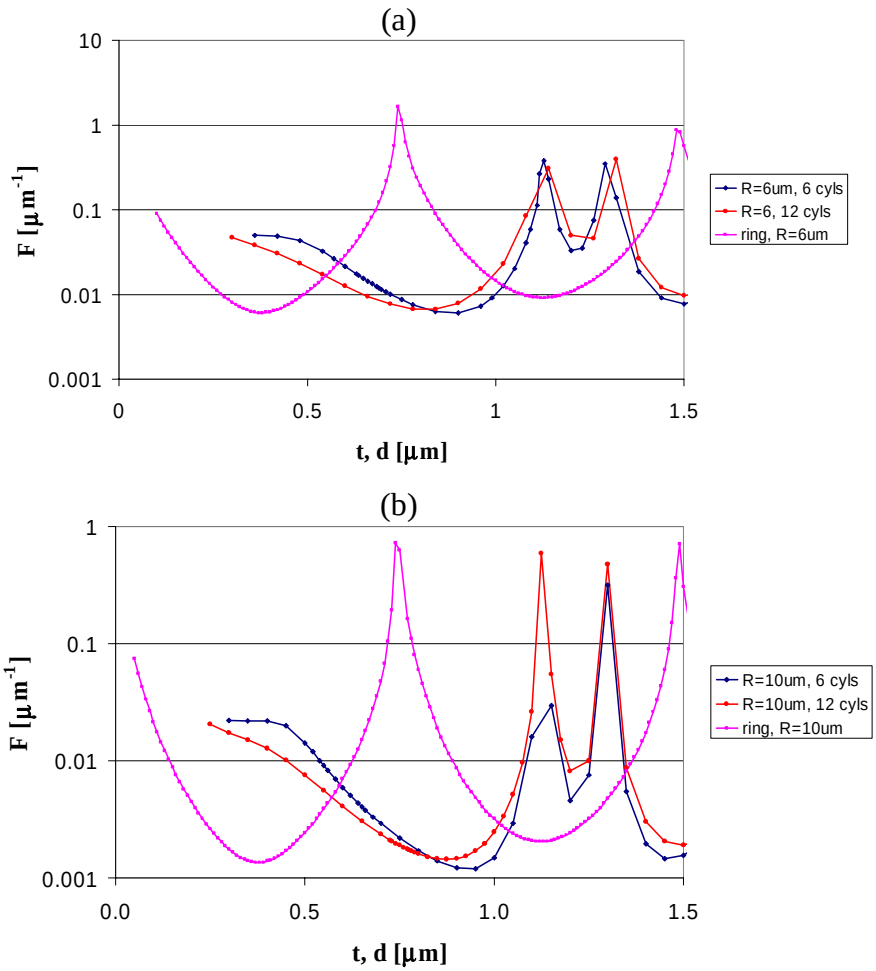


Fig. 3. (a) The normalized interface intensity for the simplified core-surround geometries.

The core-surround in a fabricated HC-PCF requires strands of silica to hold any localized antiresonant features in place. The presence of the inevitable connecting strands reduces the confining ability, changes the optimum localized feature shape (for achieving confinement) from being a cylinder, and leads to an increase in the normalized interface field intensity F. Surface tension forces which act during the fiber draw will also lead an elongation of a localized feature along the direction of the connecting strands. An appropriate geometry to consider is a number of elliptical features arranged on a thin connecting ring as shown in Fig. 4. The six ellipses have major axes of length 2*a* and minor axes of length 2*b*. The shape of the core-ring has been deformed from circular so as to connect onto the cladding with minimal deformation required in the first ring of cladding holes if the core is of 7-cell size.

#71838 - $15.00 USD Received 9 June 2006; revised 25 July 2006; accepted 26 July 2006

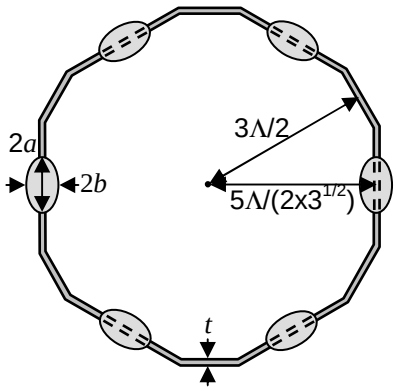


Fig. 4. A core-surround geometry which incorporates elliptical features.

Calculations of confinement loss using a boundary element code [24] indicate, in the absence of a cladding, that the connected ellipse geometry outperforms the continuous even-thickness ring geometry. Using the same code, the normalized surface field intensity F is found to be only slightly larger for the connected ellipse geometry than for the ring geometry. These findings prompted a consideration of the former geometry with a realistic cladding attached, as shown in Fig. 5(a). A stack, which is appropriate for fabricating a fiber with a geometry close to the one shown in Fig. 5(a) using the "stack-and-draw" methodology, is shown in Fig. 5(b). Solid glass rods are fused onto the inside of the central core tube at appropriately chosen positions before insertion into the stack, and surface tension forces acting during the draw are relied upon to cause elongation and merging of closely separated features to result in elliptical inclusions. An alternative fabrication scheme, which naturally produces a core surround with elliptical inclusions, has been developed [25]. It involves stacking tubes milled to a hexagonal cross-section, and a subsequent etching step [25]. This procedure, however, does not allow for easy tailoring of the ellipse size to achieve anti-resonance.

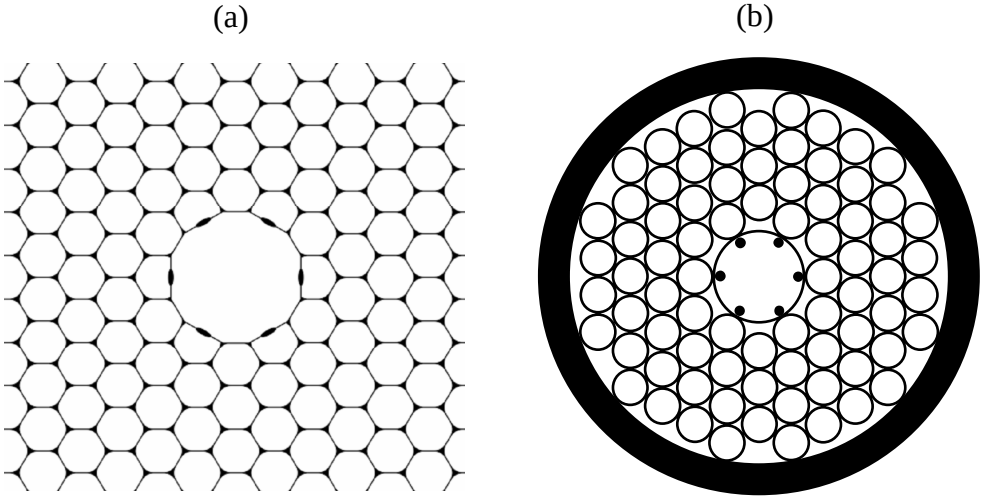


Fig. 5. (a) A HC-PCF which incorporates a core-surround of the form shown in Fig. 4(b). A stack suitable for fabricating the fiber structure shown in (a) by the stack-and-draw process using only rods and capillary tubes of circular cross-section. In practice more cladding periods than shown are incorporated to achieve sufficient light confinement.

#71838 - $15.00 USD Received 9 June 2006; revised 25 July 2006; accepted 26 July 2006

The properties of two fibers with a 7-cell core size, identical except in core-surround geometry, will be compared. Fiber A incorporates elliptical features with major-diameter length $2a=0.4\Lambda$ and minor-diameter length $2b=0.133\Lambda$ on the core-surround ring which has a thickness $t=0.031\Lambda$. Here $\Lambda$ is the cladding pitch. The core-surround of fiber B contains no elliptical features: it is simply a dodecagonal ring of thickness $t=0.031\Lambda$. The cladding structure of the fibers is defined by the unit cell shown in Fig. 6, a hole being modeled as a hexagon with rounded corners [15, 26]. The chosen values of the cladding structural parameters correspond to an air filling fraction of 91%. The minimum glass thickness in the cladding is $w=0.031\Lambda$, which equals the chosen core-ring thickness in the fibers.

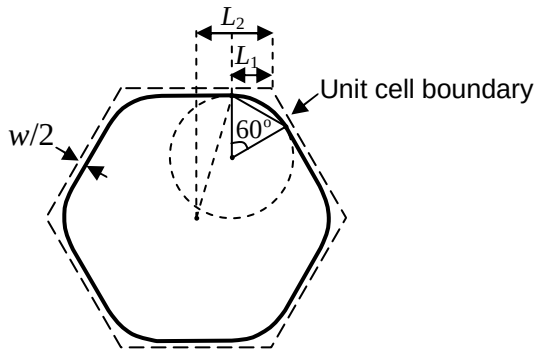


Fig 6. The geometry of a cladding unit cell. The cladding structure used for fibers A and B is defined by $L_1/L_2=0.6$ and $w=0.031\Lambda$, with $\Lambda$ the lattice pitch.

The calculations were performed using a plane-wave expansion method [27] employing a 512×512 mesh. Two different supercells were used to check convergence and adherence to $C_{6v}$ group-symmetry. One of these supercells is shown in Fig. 5(a); it is rectangular in shape, of size $10\Lambda\times6\sqrt{3}\Lambda$ and centered on the air core. The other supercell is rhombic, centered on the air core and has sides of length $10\Lambda$. It was confirmed that both choices of lead to closely matched results.

The normalized interface field intensity F for fibers A and B is shown in Fig. 7(a), plotted against normalized wavenumber $k\Lambda$ over the bandgap range where the $HE_{11}$-like mode is guided (i.e. between $k\Lambda=14.0$ and $k\Lambda=18.1$). It can be inferred that the minimum attained F for fiber A is about 3 times lower than for fiber B. This suggests fiber A should show lower loss than fiber B by a similar factor [15]. Figure 7(b) shows the light power-in-glass fraction $\eta$ for the two fibers. Despite the addition of glass associated with the elliptical features, the power-in-glass fraction for fiber A reaches a minimum value of 0.004, which is less than half the minimum $\eta$ value for fiber B. Hence the nonlinearity of fiber A will also be lower than that of fiber B.

#71838 - $15.00 USD Received 9 June 2006; revised 25 July 2006; accepted 26 July 2006

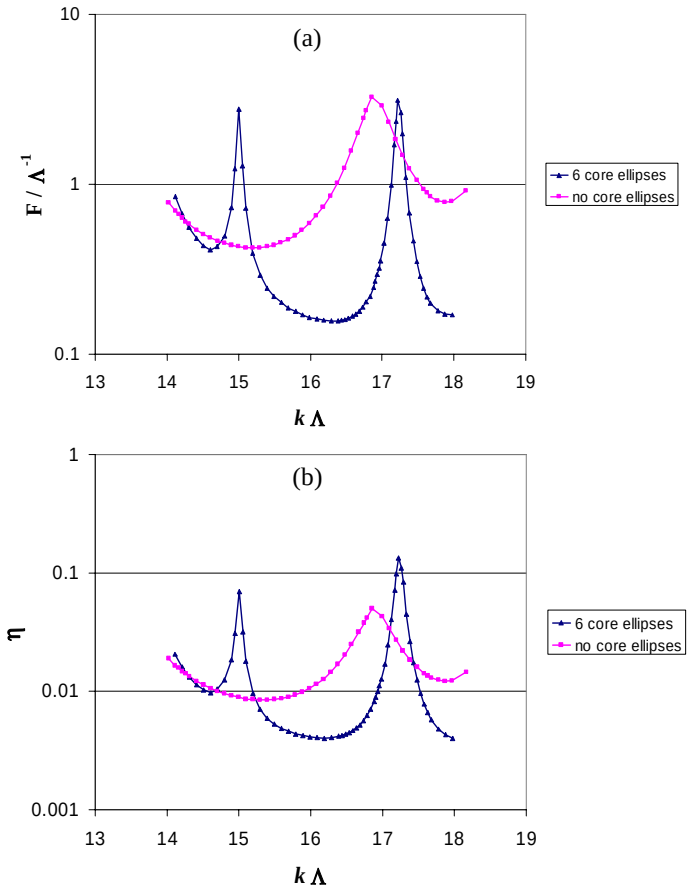


Fig. 7. (a) The normalized interface field intensity, F, and (b) the power-in-glass fraction, η, for two HC-PCFs. The blue traces are for fiber A, which incorporates elliptical features on the core surround, whereas the purple traces are for fiber B which has no such features.

The peaks in the traces of Fig. 7 are associated with anti-crossing events between the $HE_{11}$-like core mode and modes of compatible symmetry associated with the core-surround glass arrangement. The incorporation of elliptical features introduces more anti-crossing events within the band gap range, but for the 7-cell core size, low-loss propagation is still possible over a wavelength range extending over nearly 200nm centered on 1550nm. The number of unwanted anti-crossing events associated with the elliptical antiresonant core-surround inclusions is generically found to be fewer than is introduced by a continuously thick antiresonant core-surround ring such as the one considered in [16].

Computational time unfortunately prohibited a full systematic study of the mode properties as a function of the ellipse size and aspect ratio (i.e. $a$ and $b$). Similar to the influence of the thickness $t$, or radius $R$ of the ring-like core surround [25], it is found that small changes in the ellipse size or shape lead to a movement in the positions of anti-crossing events within the band gap. The chosen values $2a=0.4\Lambda$ and $2b=0.133\Lambda$ lead to a broad separation in the crossing events with the low-loss frequency range centered close to the middle of the bandgap. As such, these values of $a$ and $b$ are likely to be close to values at which a local minimum in F or η is attained.

Having identified a practical geometry which should give rise to low-loss in a non-birefringent arrangement, the next section explores birefringent designs involving elliptical inclusions on the core-surround.

#71838 - $15.00 USD Received 9 June 2006; revised 25 July 2006; accepted 26 July 2006

## 3. Low-loss birefringent designs

The simplest means of introducing birefringence to a fiber design which has localized features positioned on its core-surround ring is to remove one or more of them. Figure 8 shows a fiber in which two opposing elliptical inclusions have been removed so that polarization degeneracy is lifted, but inversion and 180° rotation symmetries remain. Except for the removal of the two ellipses, the fiber is identical to fiber A of the previous section.

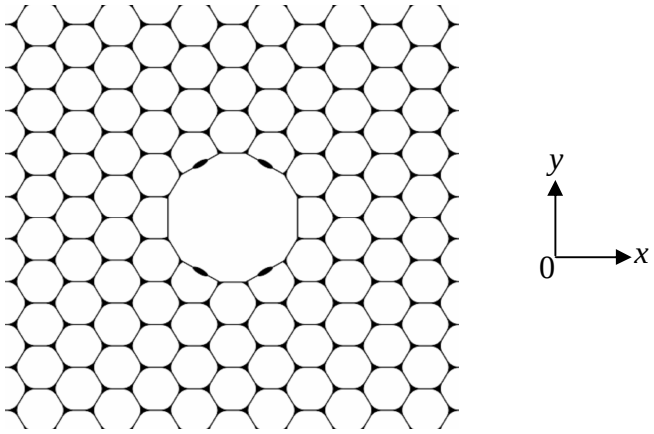


Fig. 8. A birefringent fiber design incorporating 4 elliptical features within the core surround.

The modes of the birefringent fiber were calculated using the plane wave method at 512×512 resolution, using a rectangular supercell of size $10\Lambda \times 6\sqrt{3}\Lambda$ and ensuring the inversion and 2-fold rotation symmetries are retained after the discretization.

Figure 9 shows $n_x$-$n_y$, the difference in effective index between the polarized core modes, plotted against the normalized wavenumber $k\Lambda$ over the band gap range. The index $n_x$ corresponds to the mode for which the **E**-field within the air core (and not too close to the glass interfaces) is directed along the *x*-axis as defined in Fig. 8. Similarly, $n_y$ is the index of the mode with **E**-field predominantly directed along the *y*-axis within the core. The discontinuities in the trace correspond to positions where one of the polarizations undergoes an anti-crossing event. It is seen that a very strong anti-crossing event occurs at $k\Lambda$=16.9. Over the $k\Lambda$-range 16.8-18.2, the index splitting remains above $3\times10^{-4}$ in magnitude, which should lead to strongly polarization dependent behavior.

#71838 - $15.00 USD Received 9 June 2006; revised 25 July 2006; accepted 26 July 2006

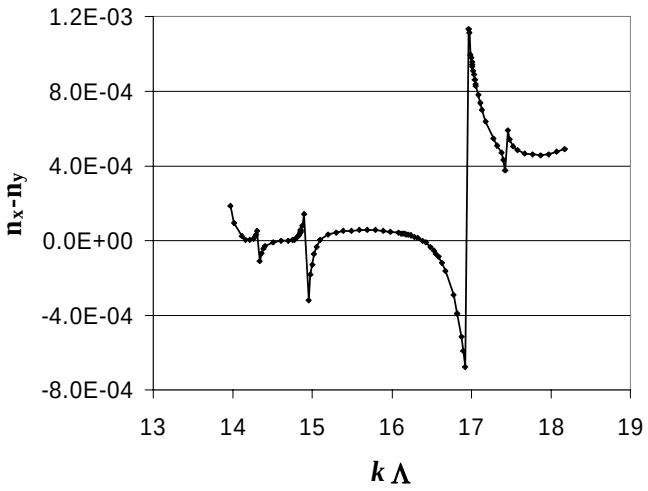


Fig. 9. The difference in effective index of the polarized modes for the birefringent HC-PCF design shown in Fig. 8.

To distinguish which polarization mode undergoes each anti-crossing and to estimate the relative loss of the polarization modes, a plot of F against normalized wavenumber $k\Lambda$ is provided in Fig. 10(a). The red curve corresponds to the mode in which most of the **E**-field is directed along 0*x* and the green curve corresponds to the mode in which most of the **E**-field is directed along *0y*, the axis directions being defined in Fig. 8. Also re-shown (blue curve) in Fig. 10 for comparison is the trace for the non birefringent design A which incorporates 6 ellipses on the core surround. Peaks in the traces correspond to anti-crossing events, which occur at different $k\Lambda$ and with different severity for the two polarization channels of the birefringent fiber [13]. The strength of the modal interactions shown by the *y*-polarized core mode between $k\Lambda$=16.2 and $k\Lambda$=17.7 is stronger than for the other polarization, which increases the value of F for this mode over the specified range. Between $k\Lambda$=15.5 and $k\Lambda$=16.8, the *x*-polarized core mode maintains a value of F which is 2 times lower than the minimum F value attained for the non-birefringent design B and only 1.5 times higher than F for design A. Around $k\Lambda$=17.5, the value of F for the *y*-polarized mode is at least 3 times higher than the value for the *x*-polarized mode, and the index splitting between the modes is above $3\times10^{-4}$. A fiber fabricated according to the current birefringent design should possess wavelength ranges where one polarization channel simultaneously shows low loss and a high degree of polarization maintenance provided: a) a birefringence level of order $3\times10^{-4}$ is sufficient to suppress cross-scattering between the polarized core modes and b) random geometric perturbations do not cause a significant coupling of the lower-loss core mode to the core-surround mode that is interacting with the higher-loss core mode. Since the loss of one polarized mode is considerably higher than the other over the ranges of high birefringence, for fiber lengths exceeding the decay length of the higher loss polarized mode, these birefringent HC-PCFs will behave as polarizing fibers. Simultaneous attainment of high birefringence and low-loss propagation of both polarizations appears to be more difficult to achieve with HC-PCFs.

The power-in-glass fraction $\eta$ for the polarized modes of the birefringent design is shown in Fig. 10(b). The minimum attained value of 0.0044 for the x-polarized mode is only slightly larger than the minimum value 0.0040 found for the non birefringent design A, implying that the nonlinearity shown by x-polarized mode is only weakly compromised by the removal of two of the elliptical features.

#71838 - $15.00 USD Received 9 June 2006; revised 25 July 2006; accepted 26 July 2006

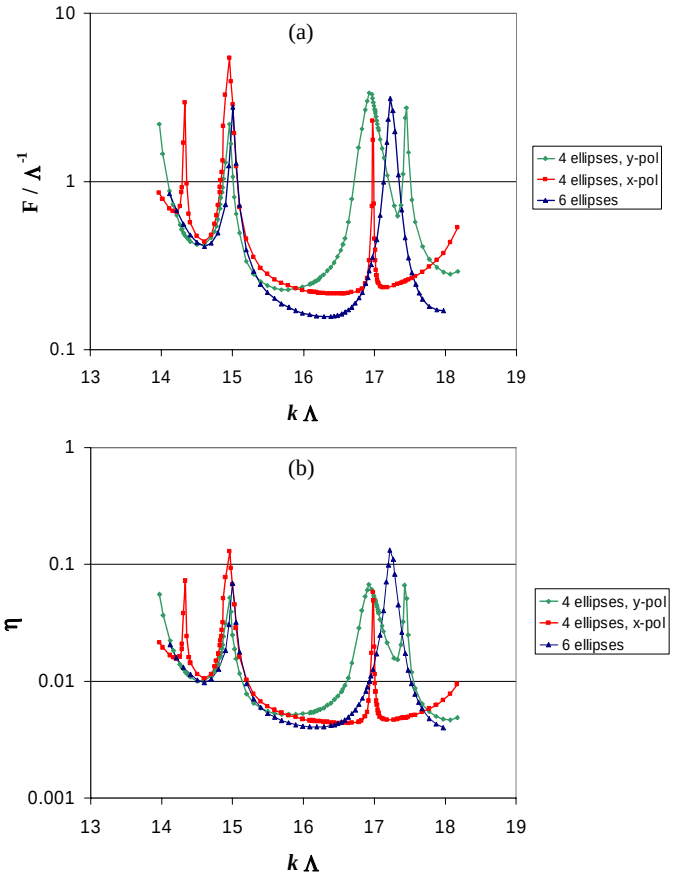


Fig. 10. (a) The normalized field intensity, F, and (b) the power-in-glass fraction, η, for the two polarized modes of the birefringent fiber with 4 core-surround ellipses. Also shown are traces for the corresponding non-birefringent fiber with 6 ellipses on the core-surround.

Figure 11 shows the logarithm of the field intensity distribution, over an 80dB range, for the two polarization modes of the birefringent fiber at normalized wavenumber $k\Lambda$=16.7. The positions of the dielectric boundaries close to the core are also shown in Fig. 11. The intensity distribution of the x-polarized mode, displayed in Fig. 11(a), shows near-nulls in the intensity close to the inner interface of the core-surround over much of its perimeter. This is an indication that an antiresonance effect remains in operation even when just 4 ellipses are incorporated within the core-surround geometry.

#71838 - $15.00 USD Received 9 June 2006; revised 25 July 2006; accepted 26 July 2006

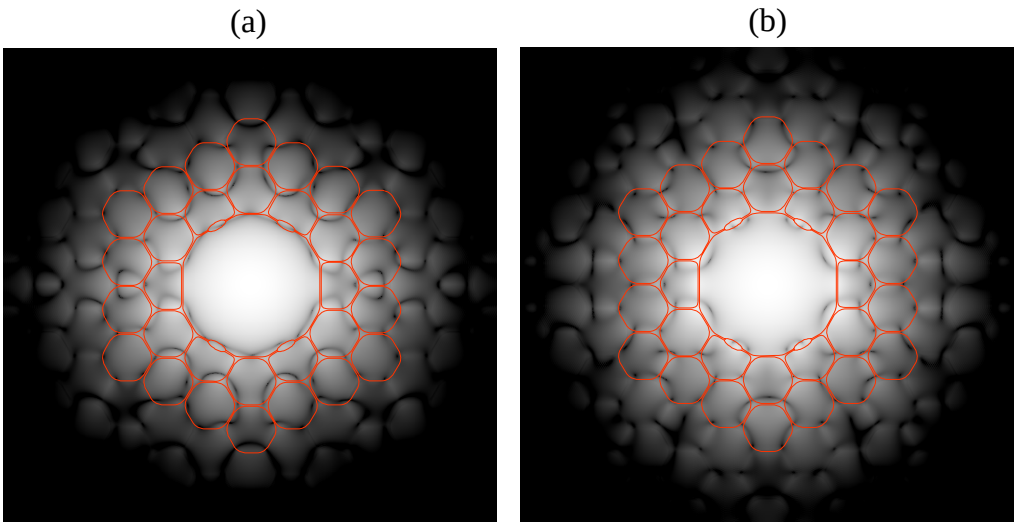


Fig. 11. The field intensity of the two polarization modes of the fiber shown in Fig. 8, calculated at the normalized $k\Lambda$=16.7. The intensity is shown on a logarithmic scale over an 80 dB range. The positions of the hole interfaces close to the core region are superimposed in red. The pattern shown in (a) is for the low-loss x-polarized mode and (b) is for the higher loss mode (y-polarized). Note that for the former mode near-nulls occur close to the core-boundary around much of its perimeter.

## 4. Conclusions

Incorporation of a number of localized features within the glass ring which surround the core of a hollow core photonic crystal fiber can significantly reduce the field intensity at the interfaces as well as the fraction of the mode power which resides within the glass. Thus such designs are candidates for showing low-loss and low nonlinearity. The improvements become manifest when the size of the localized features is tuned so that the composite core-surround geometry is rendered antiresonant within the cladding band gap. The degree of improvement that can be attained depends on the shape of the features. Inclusion of a number of elliptical features of appropriate size and aspect ratio on a thin core-surround ring has been shown to reduce the interface intensity by a factor of 3 and the power-in-glass fraction by a factor of 2. The proposed geometry is amenable to fabrication by the stack-and-draw process using just tubes and rods within the stack.

Birefringent designs have been considered which involve only 2-fold symmetric arrangements of elliptical features on the core-surround ring. High birefringence is obtained when one polarization mode is close to anti-crossing with a mode associated with the core-surround whilst the other remains free of such an interaction. The interface field intensity of the polarization mode which is clear of mode anti-crossing is sustained at a low level, which implies this polarization should show low-loss if inter-polarization mode coupling is maintained at a low level by the attendant high birefringence. Experimental and theoretical investigations are required to quantify the degree of polarization maintenance, as measured by a polarization extinction ratio, which can be achieved using these birefringent designs.

#71838 - $15.00 USD Received 9 June 2006; revised 25 July 2006; accepted 26 July 2006